Direct Measurement of Ion-Influenced Surface Diffusion

R. Ditchfield and E. G. Seebauer*

Department of Chemical Engineering, University of Illinois, Urbana, Illinois 61801

(Received 28 September 1998)

The influences of low-energy ion bombardment on surface diffusion have been quantified directly for the first time. Bombardment of germanium diffusing on silicon by noble gas ions between 15 and 65 eV affects the diffusional activation energy and preexponential factor in a strongly temperature-dependent way. Curiously, above about 850 °C the ion-influenced diffusivity actually falls below the thermal value. The results have significant implications for thin film growth by ion-assisted deposition processes. [S0031-9007(99)08397-0]

PACS numbers: 61.18.Bn, 34.50.Dy, 68.35.Fx

Irradiation-assisted thin film growth (IATFG) has become an increasingly widespread strategy for lowering deposition temperatures and improving grain size, nucleation density, film stress, and packing density. The method finds use for materials including semiconductors [1], oxides [2], nitrides [3], and carbides [4]. During ion-assisted growth, several physical phenomena occur simultaneously. These include enhanced surface diffusion, which improves film properties particularly in low-temperature applications. However, defect formation, substrate sputtering, and embedding of the bombarding gas often degrade the film [5]. Process optimization depends sensitively on the precise kinetics of all the competing phenomena.

Unfortunately, surface diffusion remains difficult to measure accurately at the temperatures that typify growth, and bombarding ions complicate the task even further. Film growth studies under conventional conditions have provided substantial indirect evidence for ion-enhanced diffusion, but no hard numbers for diffusion coefficients themselves. More fundamental work under well-characterized ultrahigh vacuum conditions is sparse [6–8] and bears only obliquely on the questions of interest in real processing. All but one of these studies have used ion energies of 1 keV or greater—too large for most growth applications. Furthermore, in no case was the diffusivity or its temperature dependence quantified [9].

This paper fills important gaps in the understanding of low-energy ion-influenced diffusion by reporting quantitative measurements for the first time. We have employed germanium absorbed on silicon as a system whose thermal diffusion behavior is well understood [10]. Furthermore, silicon-germanium alloys play an important role in applications for novel heterostructure devices [11]. We have used several different noble gas ions as the bombarding species. The results indicate that two different mechanisms operate depending on surface temperature. Significantly for film growth applications, the results demonstrate that ion bombardment does not always promote diffusion assistance but can sometimes yield inhibition.

Surface diffusion was measured in ultrahigh vacuum via optical second harmonic microscopy [10,12]. This method directly images the temporal evolution of a one-dimensional submonolayer step concentration profile that is created with a molecular beam and retractable mask. Illumination of the profile with a pulsed laser produces second harmonic generation in reflection, whose (small) yield varies with adsorbate concentration and therefore with position on the surface. Independent calibration of yield vs concentration [10] via Auger electron spectroscopy permits direct conversion of raw second harmonic images into concentration profiles. Straightforward Boltzmann-Matano analysis [12] then provides the surface diffusivity D.

Experiments were performed on atomically clean Si(111) that was p-type (B doped, 1×10^{18} cm^{-3}). Ions impinged at 60° off normal incidence from a commercial ion source (Perkin-Elmer 20-045, 2 keV) whose control electronics were modified to permit low acceleration energies between 10 and 150 V. Separate experiments with retarding filed optics in front of the surface provided precise flux and energy calibrations. The total energy spread of the beam increased linearly with acceleration voltage from 6 eV at 20 V acceleration to 16 eV at 65 V. Experiments with a movable phosphor screen in place of the surface (for current-position measurements augmented by visual inspection) showed the ion flux to be constant within 10% across the entire 1-cm sample diameter. Beam shape remained essentially independent of acceleration voltage under the conditions employed here. All experiments were performed using ion energies of 65 eV or less, where the profiles exhibited no significant desorption of Ge.

Figure 1 shows Arrhenius plots of D in experiments with Ar^+ bombardment at several energies. D exhibits conventional Arrhenius behavior, obeying the relation

$$D = D_0 \exp(-E_a/kT), \tag{1}$$

where T and k denote surface temperature and Boltzmann's constant, respectively. However, two distinct regimes appear. Below about 730 °C, D increases with increasing ion energy, but the slopes of the plots remain identical to the thermal case. At higher temperatures,

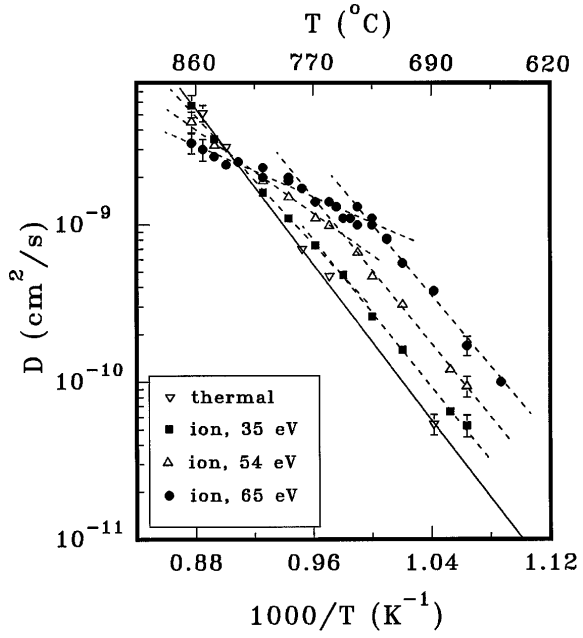

FIG. 1. Arrhenius plots for Ge diffusion under Ar^+ bombardment of 3×10^{12} ions/cm^2 s at several energies. Initial Ge converges lie near 0.6 monolayers, though diffusivities remain independent of coverage in all cases. Several typical error bars derived from standard quantitative error analysis of the diffusion profiles are shown. Lines represent least-squares fits. For comparison, thermal data also appear; the data closely match previous results [10]. The experimental domain is limited at high temperatures by the ability to heat the Si uniformly.

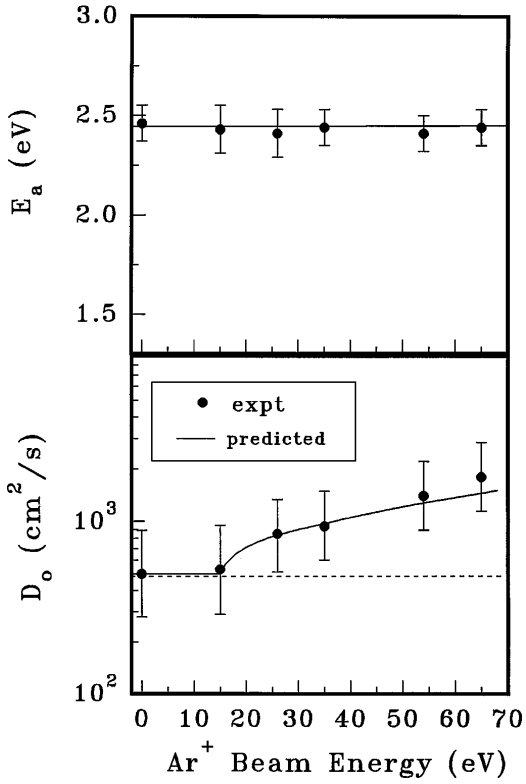

FIG. 2. Diffusional activation energies (upper panel) and preexponential factors (lower panel) obtained from Fig. 1 for the low-temperature regime. The "predicted" curve represents a fit to the form $[(E - E_{\rm crit})/E_{\rm crit}]^{1/2}$, with a threshold energy $E_{\rm crit} = 15$ eV.

the plots decrease dramatically in slope. In fact, above roughly 830 °C, D actually falls below the thermal value, signifying inhibition. The effects become more pronounced with increased energy. Experiments with different ion fluxes showed that E_a and $\log(D_0)$ vary linearly with flux in both regimes [13].

Figure 2 shows in more detail the energy dependence of E_a and D_0 obtained from data like those in Fig. 1 for $T <$ 730 °C. D_0 remains constant up to a threshold energy of 15 eV, but then increases with energy by up to a factor of 5 at 65 eV. The increase obeys the phenomenological square-root dependence of energy that is well documented for ion sputtering [5]: $[(E - E_{\rm crit})/E_{\rm crit}]^{1/2}$, shown by the line drawn for $E_{\rm crit} = 15$ eV. Other experiments (not shown) with He and Xe revealed that above $E_{\rm crit}$, D_0 increases proportionally to the square root of ion mass. Again, this dependence mirrors that observed for sputtering [5].

Above 730 °C, the behavior changes dramatically (but is not shown here). Both E_a and D_0 remain constant up to a threshold of 25 eV. Then, both E_a and $\log(D_0)$ decrease linearly with energy until reaching values of 0.96 ± 0.09 eV and $3 \times 10^{-4\pm0.3}$, respectively, at 65 eV. Again, experiments with He and Xe revealed that these quantities decrease with the square root of ion mass. Such effects do not appear to have any analog in ion sputtering.

To interpret these phenomena on an atomic level, we employed molecular dynamics simulations with a code we have used previously [10] but adapted to incorporate bombarding ions. The simulations employed a Stillinger-Weber potential [14] for the Si-Ge interaction and the repulsive part of a Morse potential for the Si-Ar and Ge-Ar interactions. Parameters for the latter potentials appear in Ref. [15].

We adjusted conditions to match the experimental setup except for the surface temperature and the ion flux, which for computational tractability we set considerably above experimental levels. The simulation temperatures lay near 80%–90% of the substrate melting temperature T_M (as opposed to 60%–70% in the experiment) in order to speed up thermal diffusion by about 5 orders of magnitude. We attempted to maintain the experimental balance of thermal and nonthermal effects by increasing the simulation fluxes by a similar factor.

Direct comparisons of simulated and experimental diffusion parameters under Ar^+ bombardment appear in Table I. We applied a scaling factor to the simulated activation energies due to computational limitations discussed previously [10]. We could incorporate only five mobile substrate layers, compared to twenty in certain other published reports [16]. It is known that small ensemble

TABLE I. Surface diffusion parameters for Ge on Si (for 65 eV Ar^+ ions at 60° off-normal incidence).

		E_a (eV)	D_0 (cm^2/s)
Low T	Sim	2.8 ± 0.2[a]	$5 \times 10^{4\pm1}$[b]
	Expt	2.44 ± 0.09	$2 \times 10^{3\pm0.3}$
High T	Sim	1.0 ± 0.2[a]	$3 \times 10^{-6\pm1}$[b]
	Expt	0.96 ± 0.09	$3 \times 10^{-4\pm0.3}$

[a]Scaled by melting temperature ratio 1683 K/2500 K [10].
[b]Scaled by ion flux ratio $3 \times 10^{12}/1 \times 10^{17}$.

sizes can lead to artificial lattice stiffening and inflated estimates of T_M [17]; indeed, our code yields T_M for Si of 2500 K [10] vs 1683 K seen experimentally. Higher melting temperatures (even apparent ones) imply stronger lattice bonding; indeed, E_a for surface self-diffusion on metals scales linearly with T_M [18]. Thus, scaling simulational energies by the ratio of the experimental T_M to the simulated one should yield the "proper" numbers for comparison with experiment [19]. Use of this procedure led to quantitative agreement between simulated and experimental surface diffusion parameters in the purely thermal case [10]. Nevertheless, both our temperature extrapolation and our scaling procedure entail risks for interpreting the interplay of thermal and nonthermal effects we describe below, and the good agreement we obtain between simulation and experiment should be viewed with due caution.

Table I shows that the computations and experiments give identical values of E_a within the error bars shown, in both the high- and low-temperature regimes. Agreement is also fairly good for D_0, although in the high-temperature regime the simulated and experimental values lie slightly outside each other's error bars. Figure 3 shows the results pictorially.

Making a connection between the molecular dynamics and the measured diffusivities requires that we recall what the experiment actually measures: the "mass-transfer" diffusivity D_M. This quantity comprises the product of the more well-known intrinsic diffusivity D_{int} and the fractional coverage θ of mobile adatoms [10,12]:

$$D_M = \theta D_{\text{int}} . \tag{2}$$

The distinction between D_M and D_{int} is important because in our experiments θ falls far below the nominal adsorbate coverage. On Si(111), adsorbates such as Ge substitute for surface Si atoms so that the most adsorbate is rendered essentially immobile [10,12]. Diffusional motion takes place via formation of adatom-vacancy pairs, in close analogy to vacancy diffusion in the bulk. The measured values for E_a and D_0 therefore contain contributions from the enthalpies and entropies of adatom-vacancy pair formation in addition to those of intrinsic motion. In fact, in thermal diffusion the enthalpy ΔH_v of pair formation composes about 1.8 of the total 2.4 eV activation energy for D_M.

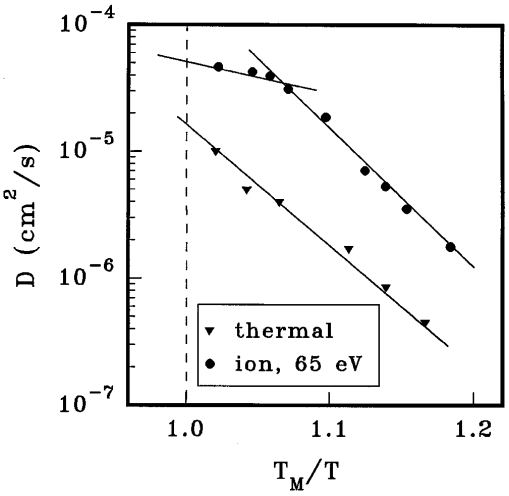

FIG. 3. Arrhenius plots obtained by molecular dynamics calculations for Ge diffusion on Si with and without Ar^+ bombardment at 65 eV, incident 60° off normal. Flux was 1×10^{17} ions/cm^2 s—4.5 orders of magnitude higher than experimental values—in order to account for the greatly increased diffusion rate at the high temperatures of the simulations. The two regimes observed in Fig. 1 appear, with similar activation energies and preexponential factors.

So in the presence of ion bombardment, what should happen to D_M? A very simple view might assume that the adatom concentration remains unaffected by ions, and that ions dislodge adatoms with an effectiveness having little or no dependence on substrate temperature. Visual inspection of simulation snapshots confirms that after direct impact from an ion, an adatom often moves two or three atomic spacings in response before rethermalizing with the underlying substrate. At very low temperatures where thermal hopping becomes slow so that ion assistance predominates, D_M should rise above its thermal value, but its activation energy should fall to ΔH_v. At very high temperatures where thermal hopping predominates, both D_M and E_a should take on their thermal values. Intermediate temperatures should yield slightly increased D_M together with slightly decreased E_a.

Interestingly, this behavior does not appear in the experimental data. D_M increases, but E_a does not decrease accordingly. Indeed, the simulations show that individual ions actually deposit very little of their energy onto the surface (1 to 2 eV out of 65 eV). Energy transfer from the ions is inefficient and may remain insufficient by itself to dislodge most adatoms. Instead, the ions may simply provide a slight additional push to adatoms possessing nearly sufficient vibrational energy to move on their own. In this view, the temperature dependence for intrinsic diffusion should not change appreciably. Only the preexponential factor should change, increasing in response to the average hop length. Since D_0 varies as the square of the hop length, which in turn increases by a factor of 2 or 3, this view predicts an increase in D_0 of 4 to 9, in accord with the parameters obtained from experiment.

At higher temperatures such assisted intrinsic diffusion continues, but a new effect becomes important. Simulations show clearly that extra adatom-vacancy pairs begin to form in response to bombardment. However, the swirl of motion in the near-surface layers that accompanies the approach of premelting at these temperatures complicates a more detailed interpretation. The data of Fig. 3 barely access the high-temperature regime, being constrained by T_M. Quantitative estimation of θ becomes difficult in this regime [10]. Nevertheless, visual inspection of the simulations reveals the continuing presence of complex and transient islanding phenomena exhibited by the purely thermal case [10]. Islands of three to ten atoms collectively nucleate out of the surface amid loosely outlined "moats" of vacancies. While dimers and trimers diffuse as units nearly as fast as monomers, the larger islands contribute to diffusion mainly by motion of attached atoms around the edges. The present simulations show no obvious change in the size, shape, or composition of these structures in response to bombardment, only in their number. It seems the ions merely provide an extra nudge to existing thermal processes in the way discussed above for intrinsic diffusion.

It is not yet completely clear why enhanced atom-vacancy pair formation should modify D_M as it does, in particular, with respect to the experimentally observed decrease. Presumably the extra vacancies serve as preferential sinks for Ge atoms as opposed to Si, so that θ in Eq. (2) ultimately decreases below its thermal value. Further efforts to quantify θ in the simulations and to trace the histories of individual Ge adatoms should clarify the picture.

This work was partially supported by NSF (CTS 98-06329). R. D. acknowledges the support of DOE (DEFG02-91ER45439) through the Materials Research Laboratory at UIUC.

*To whom correspondence should be addressed.
Electronic address: eseebaue@uiuc.edu

[1] W. Shindo and T. Ohmi, J. Appl. Phys. **79**, 2347 (1996); G. He and H. A. Atwater, Appl. Phys. Lett. **68**, 664 (1996).
[2] P. C. McIntyre, K. G. Ressler, N. Sonnenberg, and M. J. Cima, J. Vac. Sci. Technol. A **14**, 210 (1996); C. C. Li and S. B. Desu, J. Vac. Sci. Technol. A **14**, 13 (1996).
[3] I. H. Kim and S. H. Kim, J. Vac. Sci. Technol. A **13**, 2814 (1995); S. Horita, H. Akahori, and M. Kobayashi, J. Vac. Sci. Technol. A **14**, 203 (1996).
[4] Z. He, S. Inoue, and G. Carter, J. Vac. Sci. Technol. A **14**, 197 (1996).
[5] J. E. Greene and S. A. Barnett, J. Vac. Sci. Technol. **21**, 285 (1984); M. Nastasi, J. W. Mayer, and J. K. Hirvonen, *Ion-Solid Interactions: Fundamentals and Applications* (Cambridge University Press, New York, 1996).
[6] J. Y. Caville and M. Drechsler, Surf. Sci. **75**, 342 (1978).
[7] M. Drechsler, M. Junack, and R. Meclewski, Surf. Sci. **97**, 111 (1980).
[8] H. Wu, T. Fu, and T. T. Tsong, Phys. Rev. Lett. **73**, 3251 (1994).
[9] Reference [6] employed 600 eV He ions—still rather high for processing. This paper estimated diffusivities but conceded accuracy to within a factor of only 10 to 100 at best. The paper showed an Arrhenius-type sketch, but with no data points and no quotation of activation energy. Experiments were done in a field ion microscope under conditions of extremely high electric field and field gradient, muddying the mechanistic picture.
[10] C. E. Allen, R. Ditchfield, and E. G. Seebauer, Phys. Rev. B **55**, 13 304 (1997).
[11] D. H. Eaglesham, F. C. Unterwald, and D. C. Jacobsen, Phys. Rev. Lett. **70**, 966 (1993).
[12] K. A. Schultz and E. G. Seebauer, J. Chem. Phys. **97**, 6958 (1992); K. A. Schultz, I. I. Suni, and E. G. Seebauer, J. Opt. Soc. Am. B **10**, 546 (1993).
[13] These experiments employed Ar ions with flux varying by a factor of 3—the range conveniently obtainable with our setup.
[14] F. H. Stillinger and T. A. Weber, Phys. Rev. B **31**, 5262 (1985).
[15] A. A. Abrahamson, Phys. Rev. **178**, 76 (1969); D. Ostry and R. J. MacDonald, Phys. Lett. **32A**, 303 (1970); N. P. Gupta, Solid State Commun. **63**, 921 (1987); W. Eckstein, *Computer Simulation of Ion-Solid Interactions* (Springer-Verlag, New York, 1991).
[16] F. F. Abraham and J. Q. Broughton, Phys. Rev. Lett. **56**, 734 (1986); U. Landman, W. D. Leudtke, R. B. Barnett, C. L. Cleveland, M. W. Bibarsky, E. Arnold, S. Ramesh, H. Baumgart, A. Martinez, and B. Kahn, Phys. Rev. Lett. **56**, 155 (1986).
[17] A. P. Horsfield and P. Clancy, Mater. Sci. Eng. **2**, 277 (1994).
[18] H. P. Bonzel, *Structure and Properties of Metal Surfaces* (Maruzen, Tokyo, 1973).
[19] Preexponential factors require no such scaling.